Article

An asymmetric sp^3–sp^3 cross-electrophile coupling using 'ene'-reductases

https://doi.org/10.1038/s41586-022-05167-1

Received: 10 February 2022

Accepted: 3 August 2022

Published online: 11 August 2022

Check for updates

Haigen Fu[1], Jingzhe Cao[1,2], Tianzhang Qiao[1], Yuyin Qi[3], Simon J. Charnock[3], Samuel Garfinkle[2] & Todd K. Hyster[1]✉

The catalytic asymmetric construction of Csp^3–Csp^3 bonds remains one of the foremost challenges in organic synthesis[1]. Metal-catalysed cross-electrophile couplings (XECs) have emerged as a powerful tool for C–C bond formation[2–5]. However, coupling two distinct Csp^3 electrophiles with high cross-selectivity and stereoselectivity continues as an unmet challenge. Here we report a highly chemoselective and enantioselective Csp^3–Csp^3 XEC between alkyl halides and nitroalkanes catalysed by flavin-dependent 'ene'-reductases (EREDs). Photoexcitation of the enzyme-templated charge-transfer complex between an alkyl halide and a flavin cofactor enables the chemoselective reduction of alkyl halide over the thermodynamically favoured nitroalkane partner. The key C–C bond-forming step occurs by means of the reaction of an alkyl radical with an in situ-generated nitronate to form a nitro radical anion that collapses to form nitrite and an alkyl radical. An enzyme-controlled hydrogen atom transfer (HAT) affords high levels of enantioselectivity. This reactivity is unknown in small-molecule catalysis and highlights the potential for enzymes to use new mechanisms to address long-standing synthetic challenges.

Catalytic cross-couplings to forge Csp^2–Csp^2 bonds have revolutionized organic synthesis, enabling the rapid construction of molecules for the pharmaceutical and agrochemical industries[6,7]. As target compounds become more complex—correlating with a higher percentage of sp^3-hybridized atoms and stereocentres—there is a need for technologies to forge Csp^3–Csp^3 bonds stereoselectively[8,9]. XECs involving two distinct Csp^3 electrophiles are an attractive alternative to the traditional cross-couplings because they have broad functional group tolerance and avoid the need for sensitive organometallic reagents[10–12]. However, these reactions often form homo-coupled products because the metal catalysts struggle to distinguish between the two Csp^3 electrophiles. This issue can be diminished using alkyl halides that react at different rates with the metal catalyst[13,14]. Moreover, although there has been notable progress towards catalytic asymmetric Csp^2–Csp^3 XECs[4,5], stereoselective Csp^3–Csp^3 XECs are underdeveloped[15,16] (Fig. 1a). To overcome these limitations, previously unappreciated mechanistic steps and catalytic strategies need to be explored[17–19].

We questioned whether an enzyme could catalyse an asymmetric Csp^3–Csp^3 XEC. The high level of selectivity associated with biocatalytic reactions makes them attractive scaffolds for this challenge[20,21]. However, as natural enzymes do not catalyse reductive cross-coupling reactions, we needed to develop a new XEC mechanism that is compatible with existing enzymatic machinery[22,23]. Nitroalkanes are unique and ubiquitous reagents in organic synthesis but are not used as electrophiles for cross-couplings[24]. We recognized that the reactivity of nitronates could be used for a biocatalytic XEC. Nitronates react with open-shell electrophiles to forge a C–C bond and a nitro radical anion[25–28]. If this intermediate were to cleave mesolytically, the resulting radical could be quenched through HAT to afford the cross-coupled product[29]. The key to achieving this previously unknown reaction is identifying an enzyme to facilitate C–C bond formation, C–N bond mesolytic cleavage and HAT (Fig. 1b). We propose a mechanism in which reduction of the alkyl halide **1** forms an alkyl radical **4** that can react with an in situ-generated nitronate **5** to forge a new C–C bond and a nitro radical anion **6**. Enzyme-mediated homolytic cleavage of the C–N bond generates nitrite and an alkyl radical **7** that can be terminated by means of HAT to afford the cross-coupled product **3** (Fig. 1b). The proposed mechanism is attractive because the orthogonal reactivity of nitroalkanes and alkyl halides avoids undesired dimerization products.

Precise control over the chemoselectivity of the electron transfer events is required for the proposed reaction. Reduction of the nitroalkanes is thermodynamically favoured by comparison with all but the most electronically activated alkyl halides (nitroalkanes $E_{p/2} \approx -0.9$ V versus saturated calomel electrode (SCE)[30], alkyl halides $E_{p/2} = -1.1$ V to −2.5 V versus SCE[31])[32]. To achieve the desired reaction, we require a catalyst that will preferentially reduce alkyl halides instead of the nitroalkanes. We and others recently demonstrated that flavin-dependent EREDs can reduce alkyl halides using protein-templated charge-transfer (CT) complexes[33–35]. Protein-templated complexes provide the opportunity for substrate binding to override the inherent thermodynamic preference in electron transfer events. If the protein only forms the CT complex with the alkyl halide, it would be selectively reduced over the nitroalkane. Finally, EREDs can precisely control the radical-terminating

[1]Department of Chemistry and Chemical Biology, Cornell University, Ithaca, NY, USA. [2]Department of Chemistry, Princeton University, Princeton, NJ, USA. [3]Prozomix, Haltwhistle, UK. ✉e-mail: thyster@cornell.edu

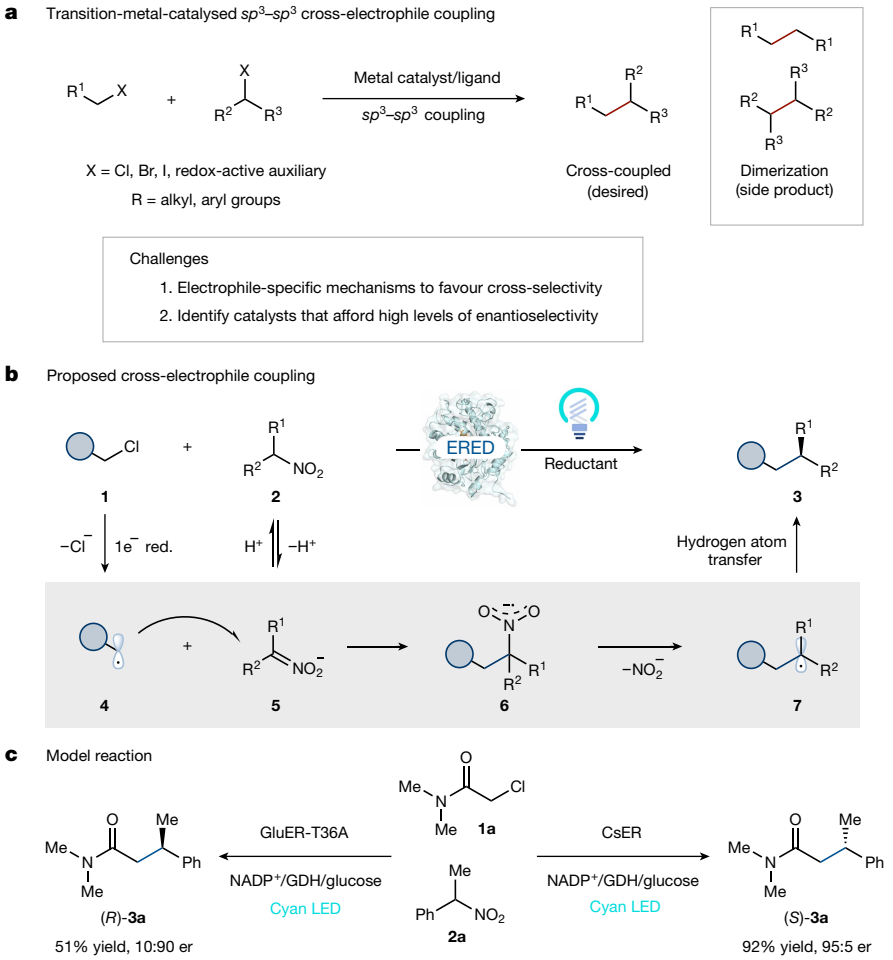

Fig. 1 | Photoenzymatic asymmetric XEC reactions. a, Challenges associated with sp^3–sp^3 XEC. **b**, Proposed photoenzymatic asymmetric XEC. **c**, Two stereocomplementary EREDs catalyse the model reaction at pH 9.0. er refers to the ratio of (*S*)-enantiomer to (*R*)-enantiomer. GDH, glucose dehydrogenase; LED, light-emitting diode; $NADP^+$, nicotinamide adenine dinucleotide phosphate.

HAT step, enabling the formation of products with high levels of enantioselectivity[36,37].

We initiated our studies by exploring the photoenzymatic coupling of α-chloroamide **1a** ($E_{p/2}$ = −1.65 V versus SCE)[33] with 1-nitroethylbenzene **2a** ($E_{p/2}$ = −0.89 V versus SCE)[30] catalysed by a panel of EREDs under cyan light irradiation (λ_{max} = 497 nm) (Supplementary Table 1). To our delight, many of the enzymes provided the desired cross-coupled product **3a** (Supplementary Table 1). The most promising catalyst was the 'ene'-reductase from *Caulobacter segnis* (CsER), providing product **3a** with moderate yield (28%) but excellent enantioselectivity, with 95:5 enantiomeric ratio (er) of (*S*)-enantiomer to (*R*)-enantiomer of the product. We suggest that the modest yield is probably owing to inadequate concentration of the nitronate at pH 8.0 (nitroalkane/nitronate = 200:1, the pK_a of **2a** is 10.3)[38]. Indeed, in moving to the more basic reaction conditions at pH 9.0 (nitroalkane/nitronate = 20:1), the desired product is formed in high yield and excellent enantioselectivity (92% yield, 95:5 er) for the (*S*)-enantiomer, outperforming other tested EREDs (Fig. 1c and Supplementary Table 2). The ERED variant from *Gluconobacter oxydans* (GluER-T36A) favours the formation of the (*R*)-enantiomer of the product (51% yield, 10:90 er), providing a complementary catalyst for accessing both enantiomers of the product (Fig. 1c). Control experiments confirmed that ERED, cyan light and NADPH (the reduced form of nicotinamide adenine dinucleotide phosphate) regeneration system (GDH/$NADP^+$/glucose) are crucial for the desired reactivity (Supplementary Table 2). Notably, this reaction can be run on a preparative scale and afford product **3a** in 72% isolated yield from a 0.10-mmol-scale reaction with no changes in enantioselectivity. We solved the crystal structure of wild-type CsER, and the docking model of **3a** with CsER suggests the (*S*)-preference of CsER in this reaction (Supplementary Fig. 4). Notably, the coupled product is not formed when the same reaction is attempted using photoredox catalysts[39]. Instead, we observed nitroalkane reduction to the oxime using $Ir(ppy)_3$ as a photoredox catalyst, highlighting that this reactivity is unique to biocatalysis.

With the optimized reaction parameters in hand, we sought to explore the scope and limitations of this photoenzymatic transformation (Fig. 2). A variety of α-aryl nitroalkanes are well accepted as XEC partners with α-chloroamide **1a**. α-Aryl nitroethanes possessing electron-donating or electron-withdrawing substituents at the *meta* and *para* positions were efficiently converted to the desired enantioenriched β-stereogenic amide products (**9**–**16**) in yields of 80–98% with excellent enantioselectivity (>97:3 er). *Ortho*-substituted α-aryl nitroalkanes were less tolerated in the reaction; only the *ortho*-fluoro-substituted nitroalkane was accepted to provide product **8** in 28% yield and 94:6 er (Fig. 2 and Supplementary Fig. 2). Furthermore, the larger substrate α-naphthalenyl nitroethane was well tolerated in this reaction, providing the corresponding product **17** with 58% yield and excellent enantioselectivity (99:1 er). This enzyme, however, was limited to relatively small alkyl substituents at the α-position. Although the ethyl group was well accepted (**19**, 64% yield and 98:2 er), larger groups, such as *n*-propyl, were poorly reactive. Pleasingly, CsER could also accommodate heterocycles, including the electron-rich

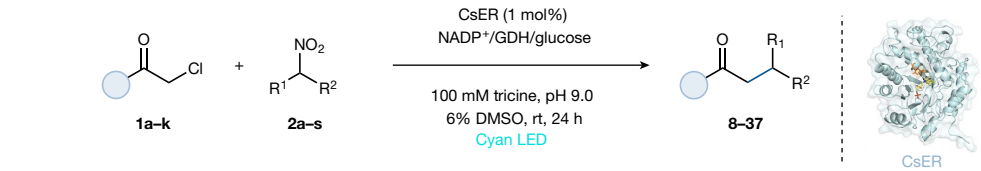

Nitroalkane scope

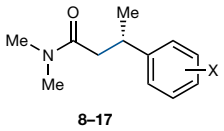

8–17

8	X = 2-F	28% yield[a], 94:6 er[b]	**13**	X = 4-OMe	96% yield, >99:1 er
9	X = 3-F	93% yield, 99:1 er	**14**	X = 4-Cl	97% (76%)[c] yield, 98:2 er
10	X = 3-Me	85% yield, 98:2 er	**15**	X = 4-Br	93% (70%) yield, 97:3 er
11	X = 3-OMe	80% yield, 99:1 er	**16**	X = 4-CF_3	98% (77%) yield, 99:1 er
12	X = 4-Me	96% yield, 98:2 er	**17**	X = 2-naphthyl	58% yield, 99:1 er

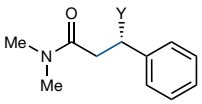

18–21

18	Y = H	28% yield
19	Y = Et	64% yield, 98:2 er
20	Y = n-Pr	15% yield, 55:45 er
21	Y = CF_3	0% yield

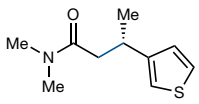

22 76% yield, 94:6 er

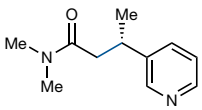

23 40% yield, 80:20 er

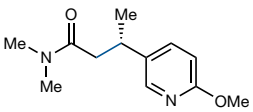

24 95% yield, 99:1 er

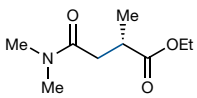

25 96% yield, 82:18 er

Alkyl halide scope

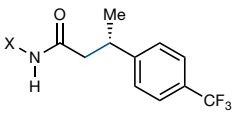

26	X = Me	75% yield, 95:5 er	**28**	X = Bn	47% yield, >99:1 er
27	X = Bn	53% yield, 87:13 er	**29**	X = OMe	53% yield, 61:39 er

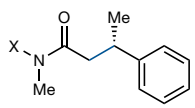

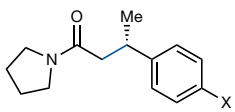

30	X = H	95% yield, 84:16 er			
31	X = CF_3	87% yield, 96:4 er			

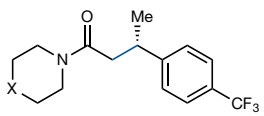

32	X = CH_2	42% yield, 85:15 er	**34**	X = H	38% yield[d], 86:14 er
33	X = O	73% yield, 91:9 er	**35**	X = CF_3	31% yield[d], 88:12 er

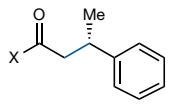

36	X = Me	54% yield, 96:4 er			
37	X = Ph	16% yield, 65:35 er			

Fig. 2 | Scope of the photoenzymatic XECs. Reaction conditions: α-chloro carbonyl substrate (10 µmol, 2 equiv), nitroalkane (5 µmol, 1 equiv), GDH-105 (0.3 mg), $NADP^+$ (0.05 µmol, 1 mol%), glucose (25 µmol) and purified ERED (0.05 µmol, 1 mol% based on nitroalkane) in tricine buffer (100 mM, pH 9.0), with 6% dimethyl sulfoxide (DMSO) as cosolvent, and the final total volume is 800 µl. Reaction mixtures were irradiated with cyan light-emitting diodes (LEDs) under anaerobic conditions at room temperature (rt) for 24 h. [a]Yields (average of duplicate) determined through liquid chromatography–mass spectrometry relative to an internal standard 1,3,5-tribromobenzene. [b]er refers to the ratio of (*S*)-enantiomer to (*R*)-enantiomer and is determined by high-performance liquid chromatography on a chiral stationary phase. [c]Isolated yields were based on 0.10-mmol-scale reaction. [d]3.0 equiv of α-bromo ester (15 µmol) were used.

α-thiophene and the electron-deficient α-pyridine nitroethanes, providing the respective β-heterocycle-substituted chiral amide products (**22**–**24**) in 40–95% yield and high enantioselectivity (up to 99:1 er). The compatibility of this photoenzyme was further highlighted by the acceptance of α-nitroester as a coupling partner, giving β-stereogenic 1,4-dicarbonyl product **25** in 96% yield and 82:18 er (Fig. 2).

As for the alkyl halide scope, secondary amides with methyl or benzyl are well accepted when coupled with α-(*p*-CF_3)phenyl nitroethane (**2j**), respectively, affording the products **26** and **27** in 75% and 53% yields and good enantioselectivities (up to 95:5 er) (Fig. 2). Tertiary amides are also well tolerated by the reaction, with cyclic pyrrolidine, piperidine, morpholine and linear Weinreb amides providing the corresponding products (**28**–**33**) in moderate to good yields and enantioselectivities (42–95% yields, up to 99:1 er). Pleasingly, different classes of carbonyls as coupling electrophiles are also feasible, as exemplified by the

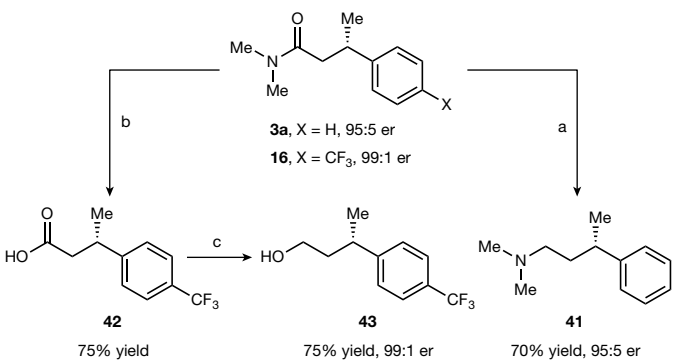

Fig. 3 | Derivatization of the enzymatic products. Reaction conditions: [a]BH_3·Me_2S (3.0 equiv), tetrahydrofuran, 0 to 65 °C, 5 h. [b]H_2SO_4 (4 M)/acetic acid, 150 °C, 16 h. [c]BH_3·Me_2S (3.0 equiv), tetrahydrofuran, 0 to 45 °C, 5 h.

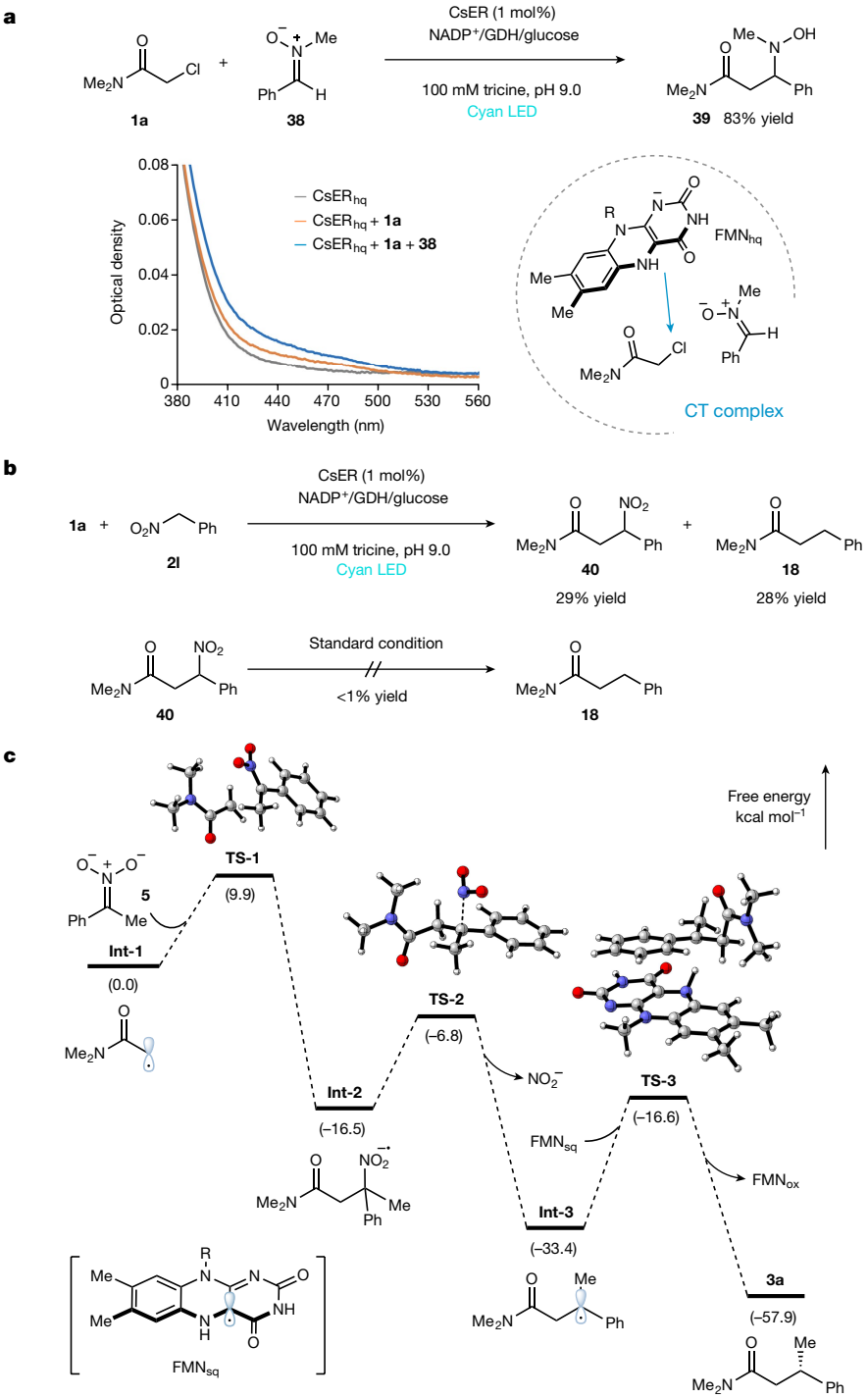

Fig. 4 | Mechanistic experiments. a, Ultraviolet–visible spectrum of reduced CsER (FMN_{hq}) in the presence of substrates. **b**, Feed experiment. **c**, DFT calculations of the model reaction. Gibbs free energies are obtained at the ωB97X-D/6-311+G(d,p)/IEFPCM//ωB97X-D/6-311+G(d,p) level of theory and are given in kcal mol^{-1}.

coupling of α-halo ester and α-halo ketones with α-aryl nitroalkanes, giving the respective enantioenriched β-chiral-substituted esters and ketones (**34**–**37**, Fig. 2). Notably, the β-chiral amide **3a** can be reduced to the corresponding γ-chiral amine **41** with good yield and no erosion of stereoselectivity (70% yield, 95:5 er, Fig. 3). Furthermore, the enzymatic product **16** can be hydrolysed to give β-chiral acid **42** and further reduced to γ-chiral alcohol **43** in good yield and excellent stereoretention (99:1 er, Fig. 3).

Mechanistic studies were conducted to determine the mode of radical initiation. Specifically, we were interested in understanding why the less oxidizing α-chloroamide (**1a**, $E_{p/2} = -1.65$ V versus SCE) is reduced preferentially to the nitroalkane (**2a**, $E_{p/2} = -0.89$ V versus SCE). We suggest that an enzyme-templated CT complex controlled the electron transfer events[33,34]. To investigate this possibility, the cofactor flavin mononucleotide (FMN) in CsER was entirely reduced to flavin hydroquinone (FMN_{hq}) with sodium dithionite, which showed negligible absorption around 500 nm (Fig. 4a). On addition of chloroamide **1a**, a new broad absorption band ($\lambda_{max} = 480$ nm) was observed, suggesting the formation of a CT complex between the FMN_{hq} and **1a**. Notably, we found that nitroalkane **2a** can oxidize the ground-state FMN_{hq} to

generate a flavin feature with an absorption band around 450–500 nm. We attribute this feature to a mixture of flavin quinone (FMN_{ox}) and flavin semiquinone (FMN_{sq}) (Supplementary Fig. 10). Notably, when nitroalkane **2a** is mixed with CsER and cofactor turnover mix under visible light irradiation, we do not observe reduction to the oxime, hydroxylamine or hydrodenitrated products. This suggests that initial reduction of the nitroalkane can occur, in contrast to examples with photoredox catalysts[39], but subsequent electron transfers to form oximes and hydroxylamines do not transpire, making this single-electron-reduction event reversible under the reaction conditions. As the first irreversible step is the reduction of the alkyl halide, reversible nitroalkane reduction does not have a detrimental effect on the reaction.

Another exciting feature of these reactions is the minimal formation of the enzyme-dependent hydrodehalogenated product (Supplementary Table 2), suggesting that alkyl halide reduction occurs when the nitronate is present in the enzyme active site. However, oxidation of FMN_{hq} by the nitroalkane obscures the observation of a higher-order CT complex (Supplementary Fig. 10). To avoid this issue, nitrone **38**, a close analogue of nitronate **5**, was used in the ultraviolet–visible spectra experiments because **38** can also readily react with **1a** (Fig. 4a), mimicking the radical initiation step of the model XEC reaction. Intriguingly, a further enhancement of the CT complex spectra was observed when nitrone **38** was added to a sample containing **1a** and the reduced CsER, indicating that a quaternary CT complex was formed to enable efficient radical formation and prolongation. No CT complex was observed using free FMN_{hq} with **1a** and **38**, suggesting that the CT complex is formed within the enzyme active site (Supplementary Fig. 11).

Next, we were interested in understanding the denitration step of the reaction. Although we propose a mechanism by which the alkyl radical reacts with the nitronate to form the unstable radical anion, which rapidly undergoes mesolytic cleavage, we recognized the possibility of a two-step mechanism in which the coupled nitroalkane is included in a redox-neutral process. The coupled nitroalkane intermediate is a substrate for reductive denitration in this scenario. To investigate this possibility, we considered the reaction using nitromethylbenzene (**2l**), which—under standard photoenzymatic conditions—forms a 1:1 mixture of cross-coupling product **18** (28% yield) and compound **40** retaining a NO_2 group (29% yield) (Fig. 4b). When the nitroalkane product **40** is resubjected to the reaction conditions, no cross-coupling product **18** was observed, indicating that the nitroalkane is not an intermediate in the denitrative coupling reaction. As nitro radical anions are proposed intermediates in non-enzymatic radical reactions but are not reported to undergo mesolytic cleavage[25,26], we postulate that the protein facilitates the mesolytic cleavage event.

The reaction with nitromethylbenzene **2l** indicates a competition between denitration and electron transfer to FMN_{sq} under the reaction conditions. To better understand the distinctive feature of this reaction, we conducted density functional theory (DFT) calculations on the model reaction (Fig. 4c) and the one involving nitromethylbenzene **2l** (Supplementary Fig. 13). We found that the initial addition step of α-amidyl radical **Int-1** to nitronate **5** is occurring rapidly with a free energy barrier of only 9.9 kcal mol^{-1} for the model reaction. The resulting radical anion **Int-2** readily undergoes irreversible denitration (a free energy barrier of 9.7 kcal mol^{-1}) to give the radical **Int-3**, which is terminated by HAT from FMN_{sq}, as supported by deuterium labelling experiments (Supplementary Fig. 8), to provide the final product **3a** (Fig. 4c). Next, the same DFT calculations were conducted with nitromethylbenzene **2l** (Supplementary Fig. 13). Although a similar free energy barrier (10.0 kcal mol^{-1}) was observed for the initial addition step, we found a higher energy barrier (13.4 kcal mol^{-1}) for the denitration step, indicating a slower denitration step when compared with the model reaction with **2a**. Thus, as a competitive pathway to the desired cross-coupling, the radical anion **Int-2′** can be terminated by oxidation by FMN_{sq} to provide product **40** (Supplementary Fig. 13).

In summary, we have established an unprecedented photoenzymatic enantioselective sp^3–sp^3 XEC between the readily available alkyl halides and nitroalkanes. This new enantioconvergent Csp^3–Csp^3 bond-formation reaction is powered by EREDs, highlighting the unparallel capability of biocatalysts in differentiating Csp^3 electrophile substrates and controlling stereoselectivity. By using non-traditional coupling partners and mechanisms, our work addresses the long-standing selectivity challenge in transitional-metal-catalysed XECs by exploiting the promiscuous unnatural reactivity of EREDs, thus expanding the biocatalyst toolbox for asymmetric C–C bond formations.

Online content

Any methods, additional references, Nature Research reporting summaries, source data, extended data, supplementary information, acknowledgements, peer review information; details of author contributions and competing interests; and statements of data and code availability are available at https://doi.org/10.1038/s41586-022-05167-1.

1. Choi, J. & Fu, G. C. Transition metal-catalyzed alkyl-alkyl bond formation: another dimension in cross-coupling chemistry. *Science* **356**, eaaf7230 (2017).
2. Everson, D. A. & Weix, D. J. Cross-electrophile coupling: principles of reactivity and selectivity. *J. Org. Chem.* **79**, 4793–4798 (2014).
3. Gu, J., Wang, X., Xue, W. & Gong, H. Nickel-catalyzed reductive coupling of alkyl halides with other electrophiles: concept and mechanistic considerations. *Org. Chem. Front.* **2**, 1411–1421 (2015).
4. Lucas, E. L. & Jarvo, E. R. Stereospecific and stereoconvergent cross-couplings between alkyl electrophiles. *Nat. Rev. Chem.* **1**, 0065 (2017).
5. Poremba, K. E., Dibrell, S. E. & Reisman, S. E. Nickel-catalyzed enantioselective reductive cross-coupling reactions. *ACS Catal.* **10**, 8237–8246 (2020).
6. Biffis, A., Centomo, P., Del Zotto, A. & Zecca, M. Pd metal catalysts for cross-couplings and related reactions in the 21st century: a critical review. *Chem. Rev.* **118**, 2249–2295 (2018).
7. Magano, J. & Dunetz, J. R. Large-scale applications of transition metal-catalyzed couplings for the synthesis of pharmaceuticals. *Chem. Rev.* **111**, 2177–2250 (2011).
8. Lovering, F., Bikker, J. & Humblet, C. Escape from flatland: increasing saturation as an approach to improving clinical success. *J. Med. Chem.* **52**, 6752–6756 (2009).
9. Lovering, F. Escape from Flatland 2: complexity and promiscuity. *MedChemComm* **4**, 515–519 (2013).
10. Qian, X., Auffrant, A., Felouat, A. & Gosmini, C. Cobalt-catalyzed reductive allylation of alkyl halides with allylic acetates or carbonates. *Angew. Chem. Int. Edn* **50**, 10402–10405 (2011).
11. Liu, J. H. et al. Copper-catalyzed reductive cross-coupling of nonactivated alkyl tosylates and mesylates with alkyl and aryl bromides. *Chem. Eur. J.* **20**, 15334–15338 (2014).
12. Sanford, A. B. et al. Nickel-catalyzed alkyl–alkyl cross-electrophile coupling reaction of 1,3-dimesylates for the synthesis of alkylcyclopropanes. *J. Am. Chem. Soc.* **142**, 5017–5023 (2020).
13. Yu, X., Yang, T., Wang, S., Xu, H. & Gong, H. Nickel-catalyzed reductive cross-coupling of unactivated alkyl halides. *Org. Lett.* **13**, 2138–2141 (2011).
14. Xu, H., Zhao, C., Qian, Q., Deng, W. & Gong, H. Nickel-catalyzed cross-coupling of unactivated alkyl halides using bis(pinacolato)diboron as reductant. *Chem. Sci.* **4**, 4022–4029 (2013).
15. Erickson, L. W., Lucas, E. L., Tollefson, E. J. & Jarvo, E. R. Nickel-catalyzed cross-electrophile coupling of alkyl fluorides: stereospecific synthesis of vinylcyclopropanes. *J. Am. Chem. Soc.* **138**, 14006–14011 (2016).
16. Tollefson, E. J., Erickson, L. W. & Jarvo, E. R. Stereospecific intramolecular reductive cross-electrophile coupling reactions for cyclopropane synthesis. *J. Am. Chem. Soc.* **137**, 9760–9763 (2015).
17. Smith, R. T. et al. Metallaphotoredox-catalyzed cross-electrophile Csp^3–Csp^3 coupling of aliphatic bromides. *J. Am. Chem. Soc.* **140**, 17433–17438 (2018).
18. Zhang, W. et al. Electrochemically driven cross-electrophile coupling of alkyl halides. *Nature* **604**, 292–297 (2022).
19. Jana, S. K., Maiti, M., Dey, P. & Maji, B. Photoredox/nickel dual catalysis enables the synthesis of alkyl cyclopropanes via $C(sp^3)$–$C(sp^3)$ cross electrophile coupling of unactivated alkyl electrophiles. *Org. Lett.* **24**, 1298–1302 (2022).
20. Bell, E. L. et al. Biocatalysis. *Nat. Rev. Methods Primers* **1**, 46 (2021).
21. Zhou, Q., Chin, M., Fu, Y., Liu, P. & Yang, Y. Stereodivergent atom-transfer radical cyclization by engineered cytochromes. *Science* **374**, 1612–1616 (2021).
22. Chatterjee, A. et al. An enantioselective artificial Suzukiase based on the biotin–streptavidin technology. *Chem. Sci.* **7**, 673–677 (2015).
23. Pierron, J. et al. Artificial metalloenzymes for asymmetric allylic alkylation on the basis of the biotin–avidin technology. *Angew. Chem. Int. Edn* **47**, 701–705 (2008).
24. Ballini, R., Bosica, G., Fiorini, D., Palmieri, A. & Petrini, M. Conjugate additions of nitroalkanes to electron-poor alkenes: recent results. *Chem. Rev.* **105**, 933–972 (2005).
25. Gildner, P. G., Gietter, A. A. S., Cui, D. & Watson, D. A. Benzylation of nitroalkanes using copper-catalyzed thermal redox catalysis: toward the facile C-alkylation of nitroalkanes. *J. Am. Chem. Soc.* **134**, 9942–9945 (2012).
26. Gietter, A. A. S., Gildner, P. G., Cinderella, A. P. & Watson, D. A. General route for preparing β-nitrocarbonyl compounds using copper thermal redox catalysis. *Org. Lett.* **16**, 3166–3169 (2014).

27. Rezazadeh, S., Devannah, V. & Watson, D. A. Nickel-catalyzed C-alkylation of nitroalkanes with unactivated alkyl iodides. *J. Am. Chem. Soc.* **139**, 8110–8113 (2017).
28. Devannah, V., Sharma, R. & Watson, D. A. Nickel-catalyzed asymmetric C-alkylation of nitroalkanes: synthesis of enantioenriched β-nitroamides. *J. Am. Chem. Soc.* **141**, 8436–8440 (2019).
29. Kornblum, N., Carlson, S. C. & Smith, R. G. Replacement of the nitro group by hydrogen. *J. Am. Chem. Soc.* **100**, 289–290 (1978).
30. Tanner, D. D. et al. The mechanism of the radical chain transformation of nitroalkanes to alkanes using triaryl- or trialkyltin hydrides. *J. Org. Chem.* **55**, 3321–3325 (1990).
31. Roth, H. G., Roth, H. G., Romero, N. A. & Nicewicz, D. A. Experimental and calculated electrochemical potentials of common organic molecules for applications to single-electron redox chemistry. *Synlett* **27**, 714–723 (2016).
32. Durchschein, K. et al. Reductive biotransformation of nitroalkenes via nitroso-intermediates to oxazetes catalyzed by xenobiotic reductase A (XenA). *Org. Biomol. Chem.* **9**, 3364–3369 (2011).
33. Biegasiewicz, K. F. et al. Photoexcitation of flavoenzymes enables a stereoselective radical cyclization. *Science* **364**, 1166–1169 (2019).
34. Page, C. G. et al. Quaternary charge-transfer complex enables photoenzymatic intermolecular hydroalkylation of olefins. *J. Am. Chem. Soc.* **143**, 97–102 (2020).
35. Huang, X. et al. Photoenzymatic enantioselective intermolecular radical hydroalkylation. *Nature* **584**, 69–74 (2020).
36. Fu, H. et al. Ground-state electron transfer as an initiation mechanism for biocatalytic C–C bond forming reactions. *J. Am. Chem. Soc.* **143**, 9622–9629 (2021).
37. Sandoval, B. A., Meichan, A. J. & Hyster, T. K. Enantioselective hydrogen atom transfer: discovery of catalytic promiscuity in flavin-dependent 'ene'-reductases. *J. Am. Chem. Soc.* **139**, 11313–11316 (2017).
38. Fukuyama, M. et al. Thermodynamic and kinetic acidity properties of nitroalkanes. Correlation of the effects of structure on the ionization constants and the rate constants of neutralization of substituted 1-phenyl-1-nitroethanes. *J. Am. Chem. Soc.* **92**, 4689–4699 (1970).
39. Cai, S., Zhang, S., Zhao, Y. & Wang, D. Z. New approach to oximes through reduction of nitro compounds enabled by visible light photoredox catalysis. *Org. Lett.* **15**, 2660–2663 (2013).

Data availability

The data supporting the findings in this study are available within the paper and its Supplementary Information. Crystallographic models and structure factors have been deposited in the Protein Data Bank with accession number 7TNB for CsER.

Acknowledgements We thank P. Jeffrey for assistance with X-ray structure determination and the staff of NSLS-II beamline AMX (17-ID-1) for help with data collection. We thank the Stache group and the Musser group for use of their equipment and the Collum group for use of their computational resources. We thank Y. Zheng for assistance with docking and S. Sun and J. Turek-Herman for discussion. The research reported here was supported by the NIH National Institute of General Medical Sciences (R01GM127703). This work made use of the Cornell University NMR Facility, which is supported, in part, by the NSF through MRI award CHE-1531632.

Author contributions H.F. and J.C. performed and analysed the experiments. T.Q. performed the DFT calculations. Y.Q. and S.J.C. performed metagenomic mining and prepared the CsER enzyme. S.G. collected the crystallographic data of CsER. H.F. and T.K.H. designed the experiments. T.K.H. directed the project. The manuscript was prepared with feedback from all the authors.

Competing interests S.J.C. and Y.Q. are employed by Prozomix, the company that provided the sequence for CsER. The other authors declare no competing interests.

Additional information
Supplementary information The online version contains supplementary material available at https://doi.org/10.1038/s41586-022-05167-1.
Correspondence and requests for materials should be addressed to Todd K. Hyster.
Peer review information *Nature* thanks the anonymous reviewers for their contribution to the peer review of this work.
Reprints and permissions information is available at http://www.nature.com/reprints.